

Eighth WMO International Workshop on Monsoons (IWM-8) 17-21 March 2025, Pune, India

"Advancing the Understanding & Prediction of Monsoons and their
Impacts in a Changing Climate"

WORKSHOP THEMES →

Robust Intensification of the Monsoon Somali Jet under Global Warming

R. Krishnan, Aswin Sagar, T.P. Sabin

Indian Institute of Tropical Meteorology, Pune, India



Ministry Of Earth Sciences
Government of India

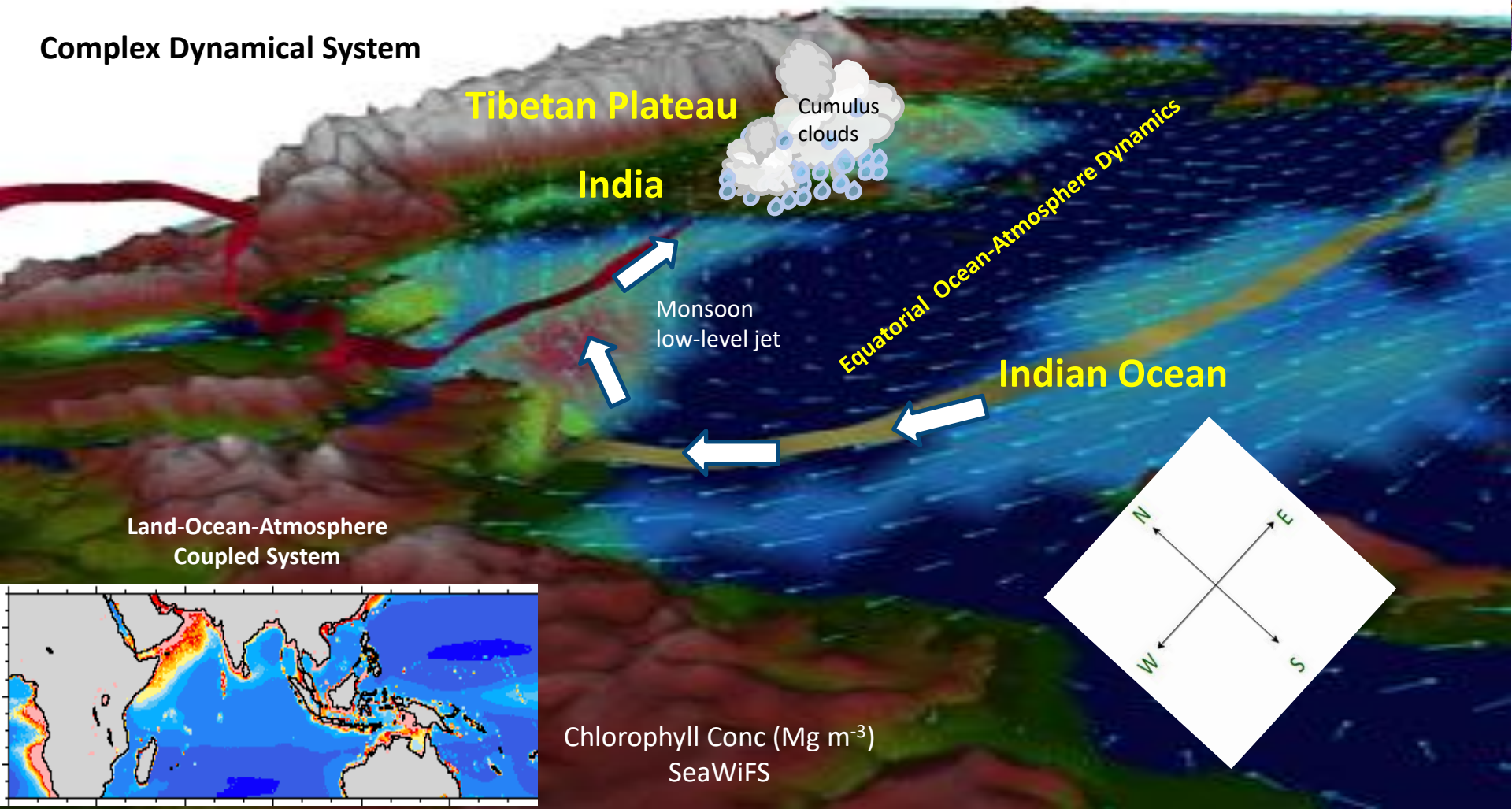


WORLD
METEOROLOGICAL
ORGANIZATION



The Indian Summer Monsoon

Complex Dynamical System



Global and regional monsoon domains

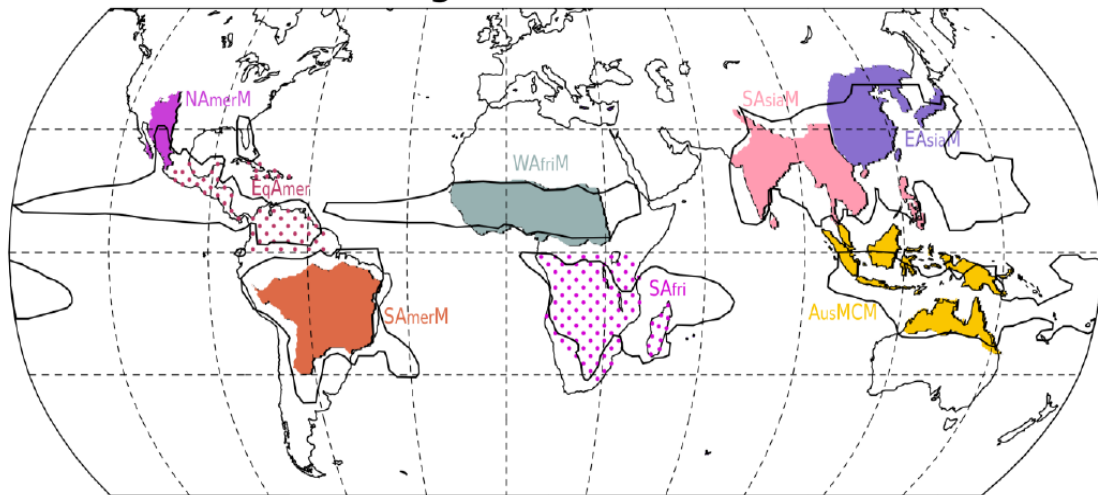


Figure AV.1 - **Annex V: Monsoons**

Global (black contour) and regional monsoons (color shaded) domains. The global monsoon (GM) is defined as the area with local summer-minus-winter precipitation rate exceeding 2.5 mm day^{-1} .

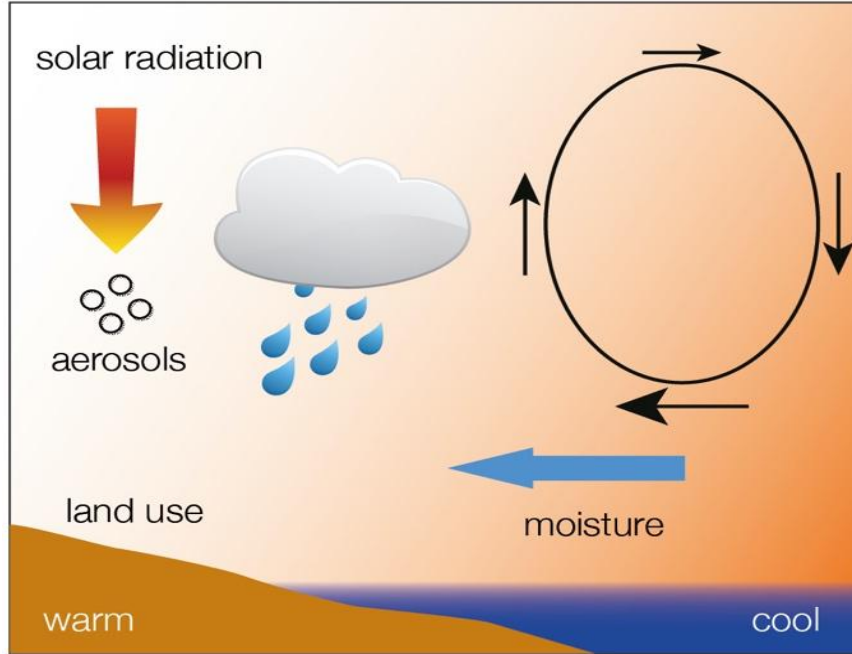
Box TS.13: Monsoons

- **Global land monsoon precipitation decreased from the 1950s to the 1980s**, partly due to anthropogenic aerosols, but has increased since then in response to GHG forcing and large-scale multi-decadal variability (*medium confidence*).
- **During the 21st century, global land monsoon precipitation is projected to increase** in response to GHG warming in all time horizons and scenarios (*high confidence*).
- **In the long-term (2081-2100), global monsoon rainfall change will feature a robust north-south asymmetry** characterized by a greater increase in the Northern Hemisphere than in the Southern Hemisphere and **an east-west asymmetry** characterized by enhanced Asian-African monsoons and a weakened North American monsoon (*medium confidence*).
- **Northern Hemispheric monsoon circulation will likely weaken over the 21st century** (Lee et al., 2021) – IPCC AR6 Ch4

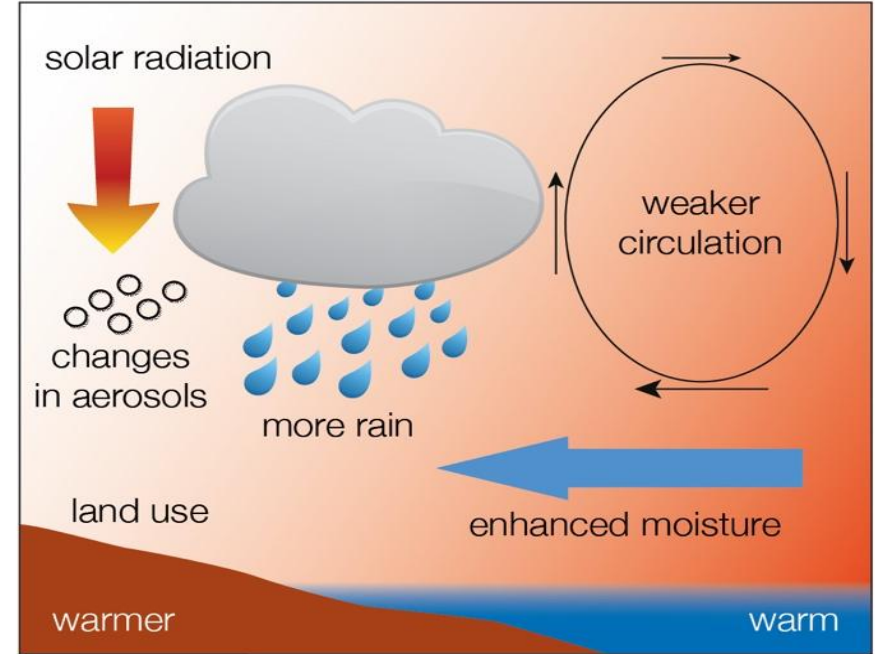
**How will the Indian summer monsoon
precipitation and circulation respond to
global warming ?**

*Simplified illustration of the influence of climate change on monsoon **rainfall & circulation***

(a) present



(b) future

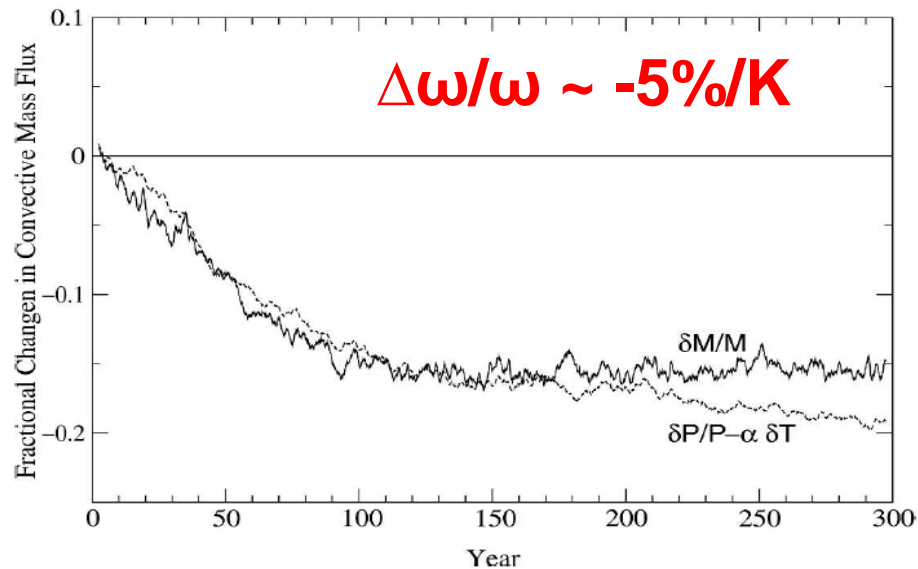
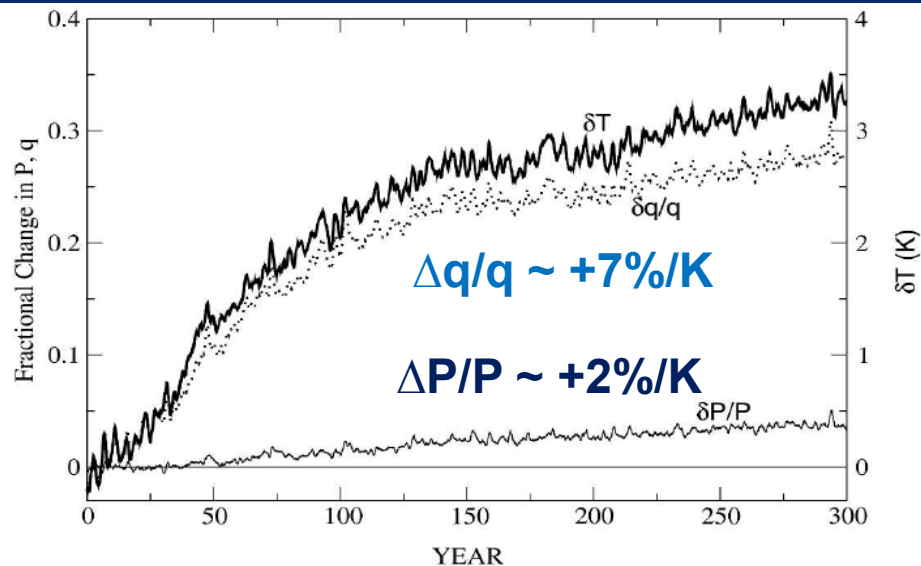


Caption: Schematic diagram illustrating the main ways that human activity influences monsoon rainfall. As the climate warms, increasing water vapour transport from the ocean into land increases because warmer air contains more water vapour. This also **increases the potential for heavy rainfalls**. **Warming-related changes in large-scale circulation influence the strength and extent of the overall monsoon circulation**. Land use change and atmospheric aerosol loading can also affect the amount of solar radiation that is absorbed in the atmosphere and land, potentially moderating the land–sea temperature difference. **Source: IPCC AR5**

Physics behind weakening circulation but more precipitation

$$P = \omega q; \frac{\Delta P}{P} = \frac{\Delta q}{q} + \frac{\Delta \omega}{\omega}$$

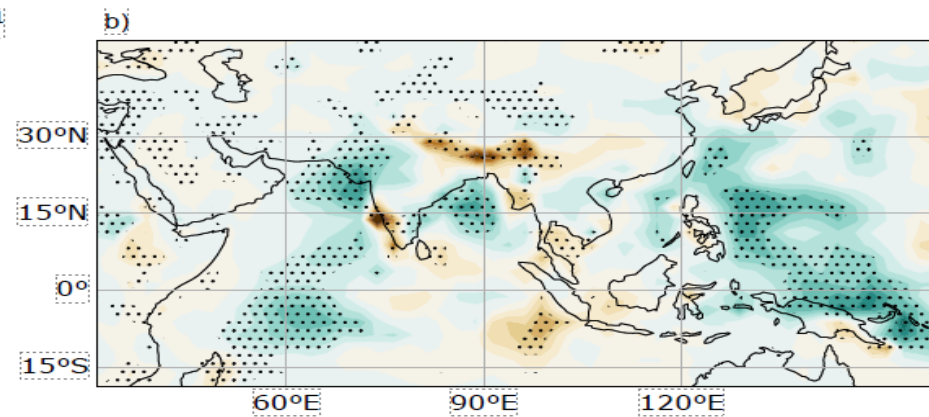
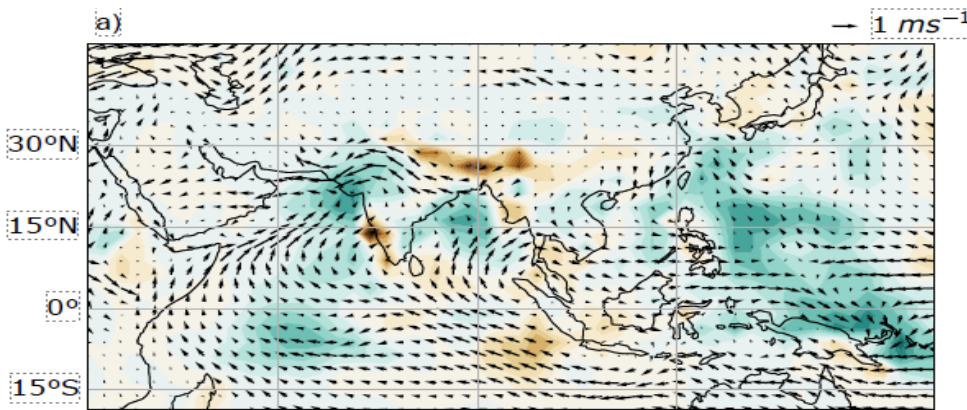
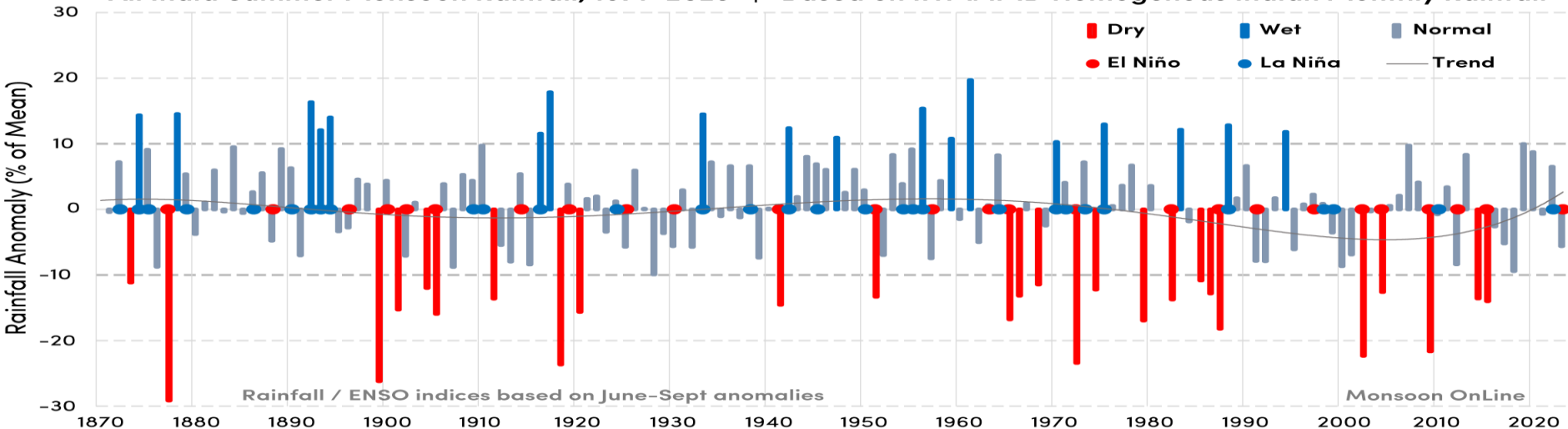
Valid for closed domains



Held and Soden, 2006

All India Summer Monsoon Rainfall, 1871–2023

Based on IITM/IMD Homogeneous Indian Monthly Rainfall



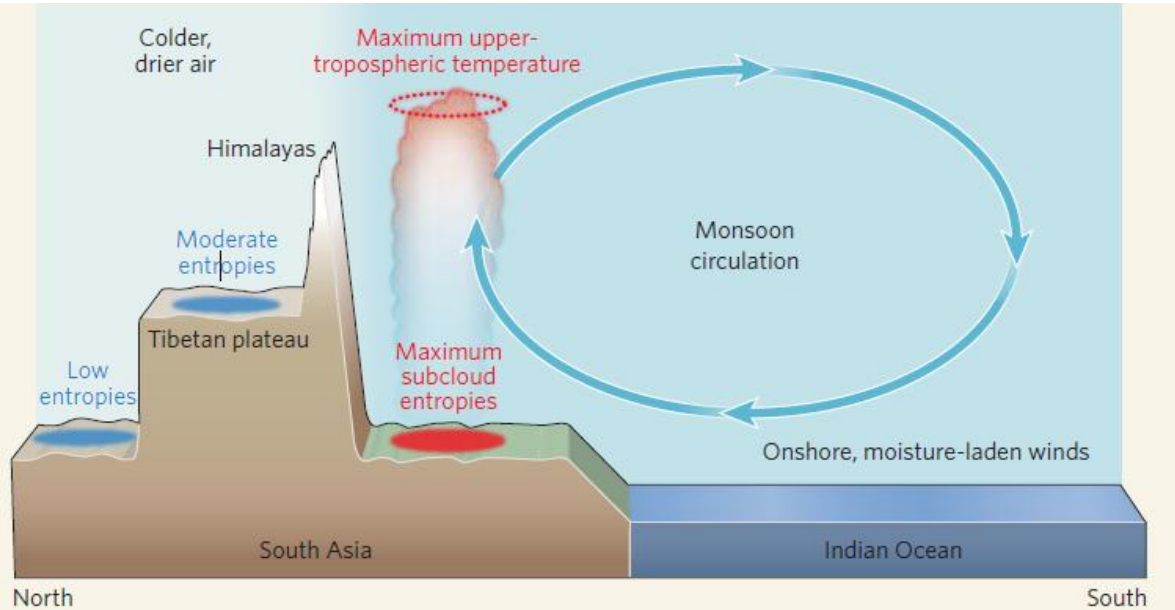
Difference map of precipitation and winds from GPCP and ERA5 datasets between (2003–2020) and (1979–2002) (a) Precipitation (shading: mm day⁻¹) and 850 hPa winds (vector: m s⁻¹), (b) Precipitation with statistical significance ($p < 0.01$) shown by stippling

A moist model monsoon

Nature News & Views 2010

Mark A. Cane

Received wisdom about the main driver of the South Asian monsoon comes into question with a report that tests the idea that the Himalayas, not the Tibetan plateau, are the essential topographic ingredient.



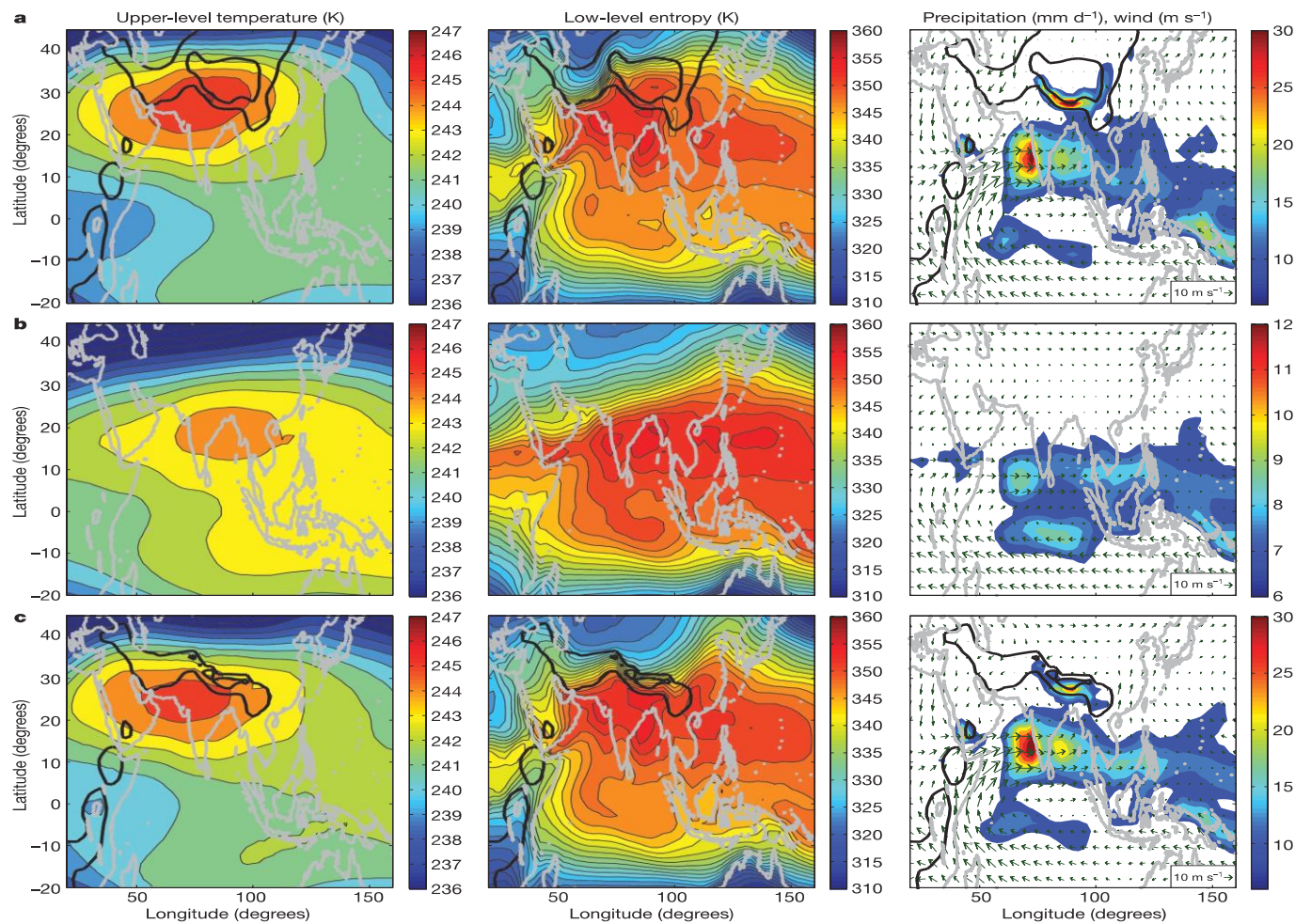
Convective Quasi Equilibrium (CQE) Framework

- Moist convective systems are in statistical equilibrium with their environment
- Virtual temperature of the free atmosphere is directly linked to subcloud-layer entropy

Ref:

- Arakawa and Schubert, 1974, J.Atmos.Sci
- Emanuel, K.A., Neelin, DJ, Bretherton, CS, QJRM, 1994
- Arakawa and Cheng, 1993, Met. Monograph
- Emanuel, K.A., 1995, J.Atmos.Sci.
- Prive and Plumb, 2007, J.Atmos.Sci
- Nie, J., Boos,WR, Kuang, Z, 2010, J.Clim

Figure 1 | A new model monsoon. Boos and Kuang's thinking centres on the role of moist convection rather than heat absorbed and radiated by the Tibetan plateau. Maximum subcloud moist entropy occurs south of the Himalayas, and the heat released as water vapour rises and condenses is reflected in peak temperatures in the overlying upper troposphere. The Himalayas keep the moist warm air over South Asia separated from the colder, drier air to the north, so the high energy of this air mass is undiluted, remains favourable for moisture-driven convection and underlies the strength of the South Asian monsoon.



*Present-day
topography*

Importance of the
Himalaya, but not
Tibet

No topography

*No Tibet, but with the
Himalaya (& east Africa)*

[Boos and Kuang 2010]

175-450 mb Temperature

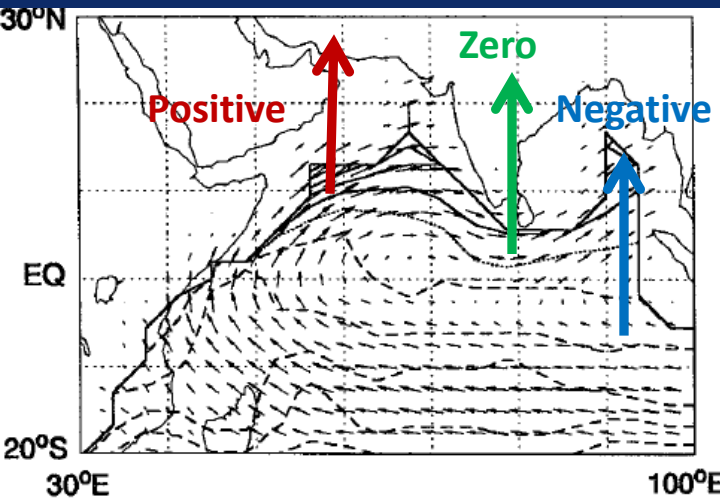
subcloud θ_{eb}

Precipitation and winds:

all for summer

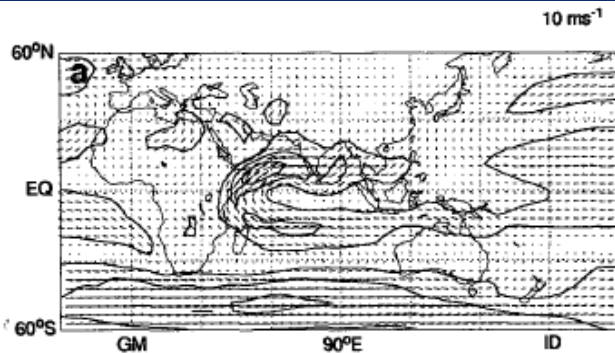
(moist static energy)

Time-mean JJA fields ECMWF analyses (1983-1988)

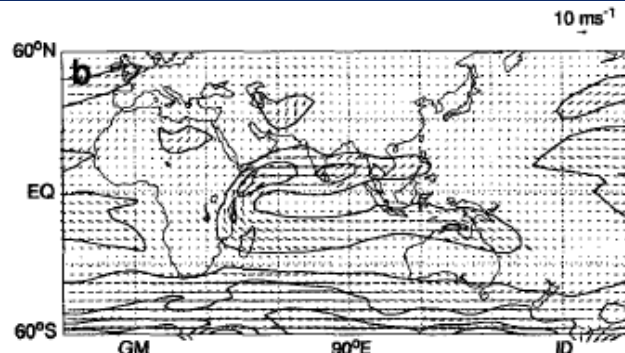


PV and horizontal wind vectors on the 302 K isentropic surface.
Contour interval is 0.05 PV units.

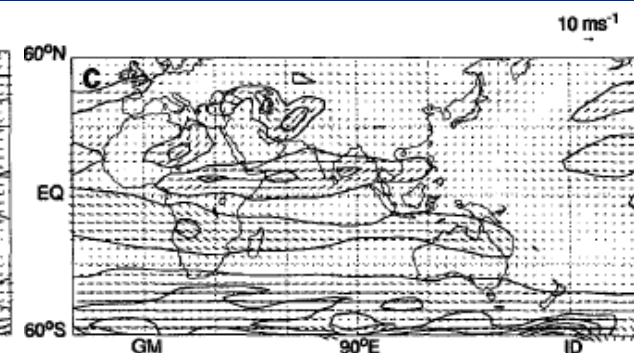
ECMWF Analyses: 887 hPa winds & isotachs



Standard Integration (Day 14)



Experiment Without (East African Highlands and Land/Sea Contrast in Surface Friction) (Day 14)



A Model of the Asian Summer Monsoon.

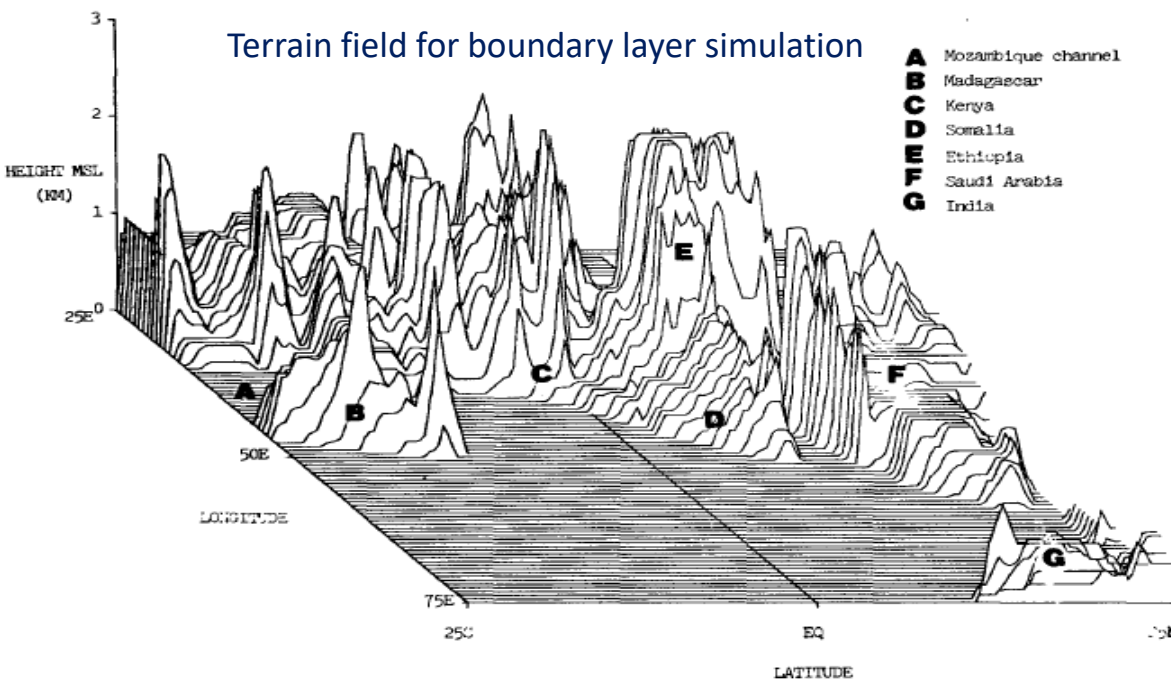
Part II: Cross-Equatorial Flow and PV Behavior

Mark J. Rodwell and Brian J. Hoskins (J. Atmos.Sci 1995)

Mechanisms that sustain the low-level East African Jet

- The East African Highland and a land/sea contrast in surface friction are essential for the existence and concentration of cross-equatorial flow
- Surface friction and local diabatic heating provide mechanisms for material modification of PV and both are important for the maintenance of the jet

Terrain field for boundary layer simulation



A Three-Dimensional Planetary Boundary Layer Model for the Somali Jet – T. N. Krishnamurti et al., 1982 J. Atmos. Sci

Mesoscale fine mesh model, with a horizontal resolution of ~ 55 km and a vertical resolution of 200 m, is integrated to examine the evolution of the 3D planetary boundary layer flows for prescribed 3-D pressure patterns.

This study examined the balance of forces in the surface layer and the planetary boundary layer for regions across the equator, across and along the low-level Somali jet, and across an Intertropical convergence zone.

The important role of advective accelerations in the near-equatorial balance of forces was demonstrated.

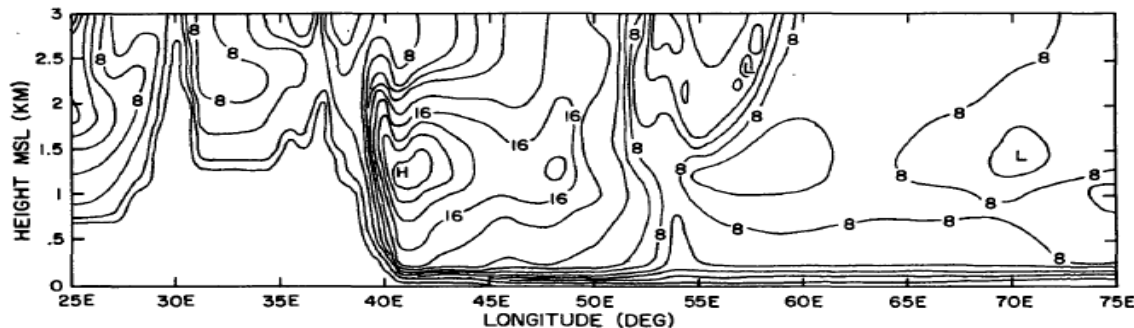


FIG. 12. Vertical-zonal cross-section of the meridional wind (m s^{-1}) along 2°S for the MONSOON 1977 simulation at day 18.

Annual intensification of the Somali jet in a quasi-equilibrium framework: Observational composites

William R. Boos^{a*} and Kerry A. Emanuel^b

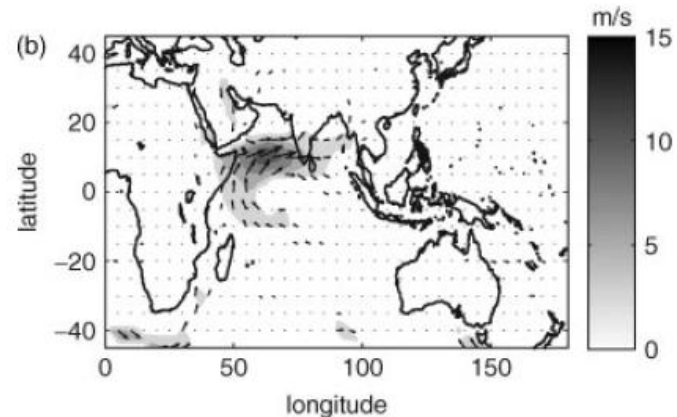
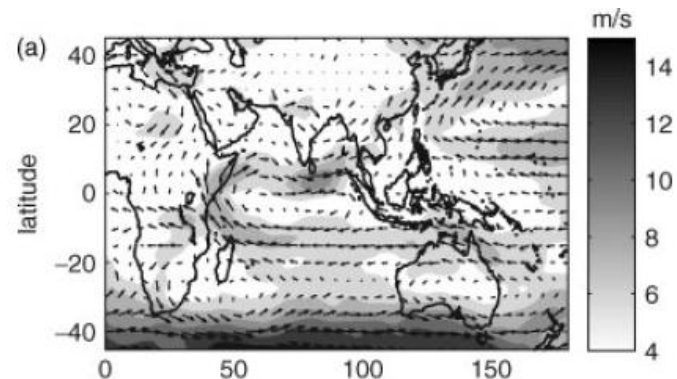
^aDept. of Earth and Planetary Sciences, Harvard University, Cambridge, Mass, USA

^bProgram in Atmospheres, Oceans, and Climate, Massachusetts Institute of Technology, Cambridge, Mass, USA

ABSTRACT: The annual intensification of the Somali jet, which accompanies the onset of the Indian summer monsoon, is rapid compared to the evolution of the seasonal insolation forcing. Using observationally-based data sets, the dynamic and thermodynamic changes accompanying the onset of this jet are presented. The abrupt component of jet onset is shown to occur over ocean about 1000 km east of the East African highlands, and is accompanied by increases in both deep convection and baroclinic flow over the off-equatorial Arabian Sea. These abrupt changes are well separated from the core of the cross-equatorial jet, which is located over land adjacent to the East African highlands.

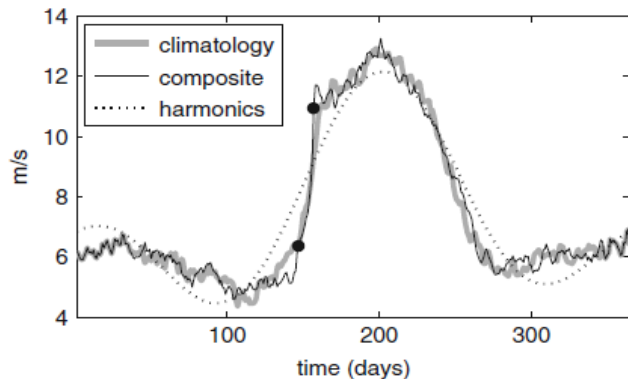
The onset of the Somali jet and the associated monsoon are then examined in a convective quasi-equilibrium framework. Such a framework is consistent with the mean summer state, in that peak free-tropospheric temperatures are nearly collocated with peak subcloud layer entropies over the northern Bay of Bengal and adjacent coastal regions. Jet onset is accompanied by a large ($O(100 \text{ W m}^{-2})$) increase in surface enthalpy flux over the Arabian Sea that is nearly collocated with, and linearly related to, the concurrent increase in deep tropospheric ascent. At the same time, the highest subcloud entropies shift inland slightly from the Bay of Bengal, and the region of warmest free-tropospheric temperatures expands poleward. The consistency of all of these changes with a wind–evaporation feedback and several other hypothesized mechanisms of abrupt monsoon onset is discussed. Copyright © 2009 Royal Meteorological Society

Boos and Emanuel, 2009

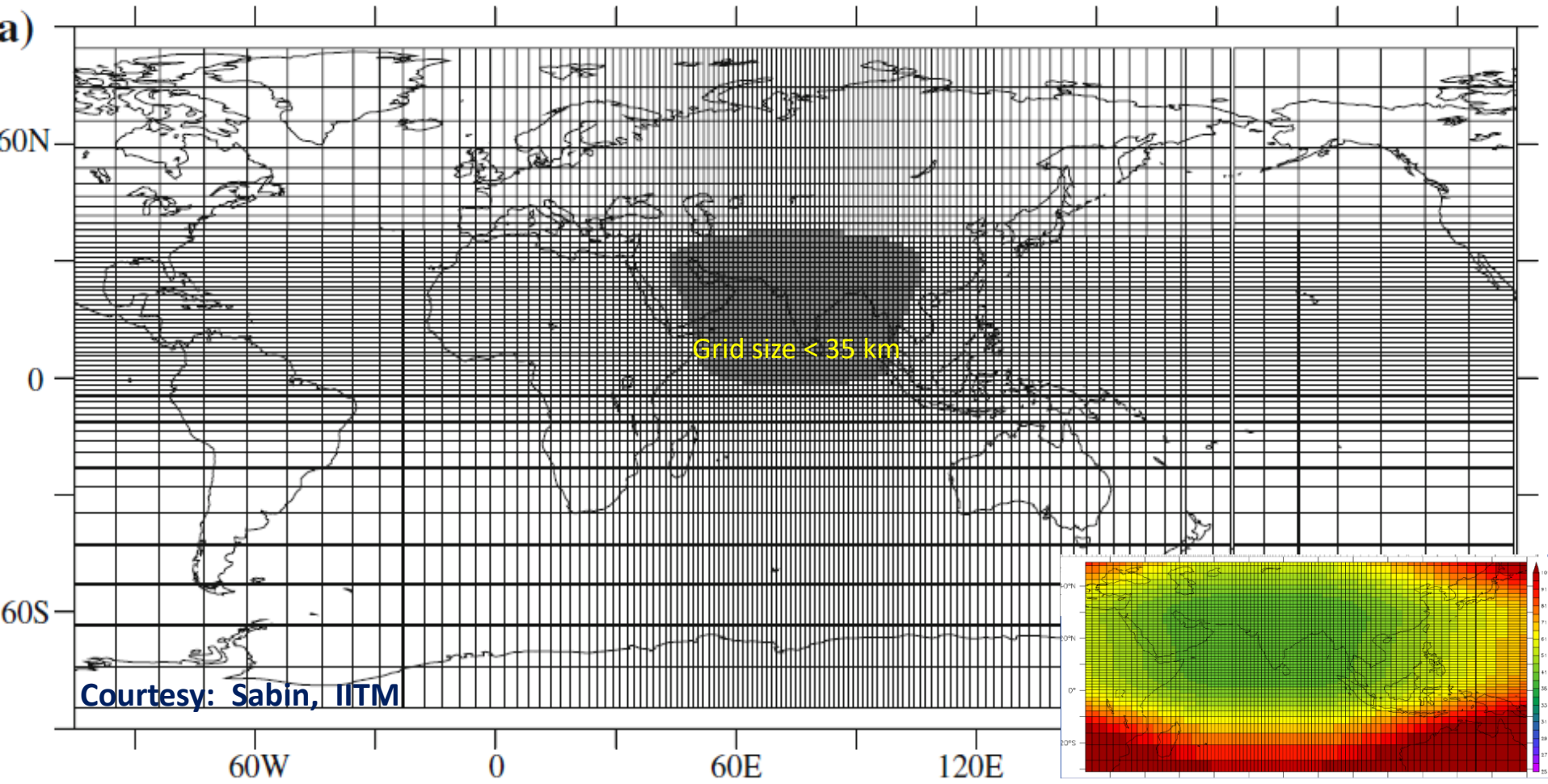


NCEP vector wind at 850 hPa (arrows). (a) is a composite 10 days before the date of jet onset, and (b) is the composite change in vector wind over the 10-day period preceding jet onset. In both panels, the shading denotes the magnitude of the wind vector (ms^{-1}), not the change. Areas with surface pressure less than 850 hPa are masked out.

Annual cycle of the jet speed index in 27 years of the NCEP reanalysis. The black line represents the composite evolution relative to the date of jet onset, the grey line is a calendar-based climatology, and the dotted line is the best fit of the first two Fourier harmonics of Earth's annual cycle to the composite. Time is the number of days since 1 January, with the composite time series shifted so that jet onset occurs at day 156, the mean onset date. The two black dots are positioned at the day of onset and 10 days prior to onset.

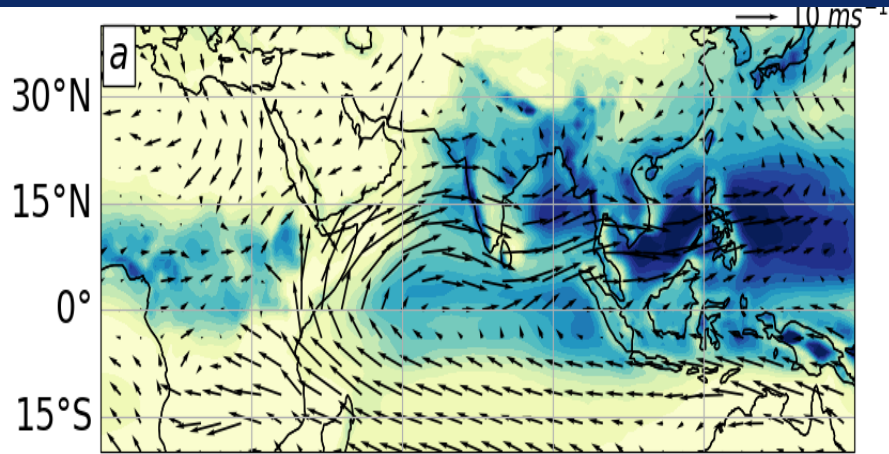


LMDZ variable resolution global atmospheric model with zooming over South Asia

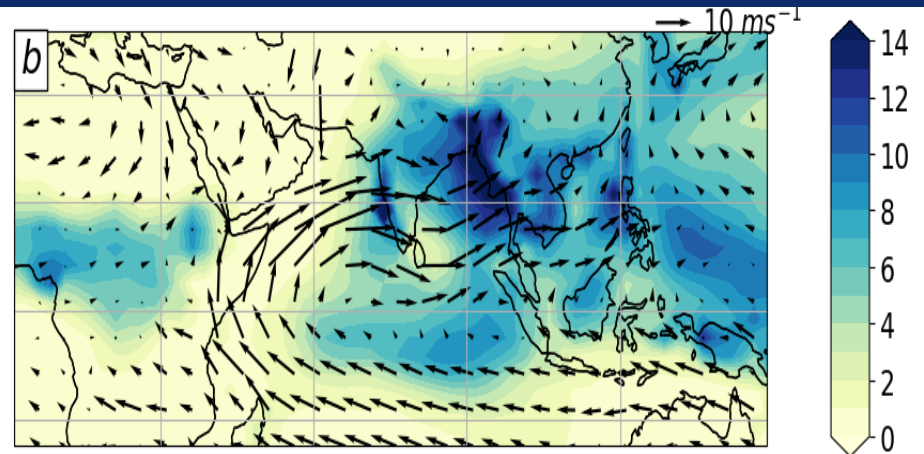


JJAS mean rainfall and 850 hPa winds

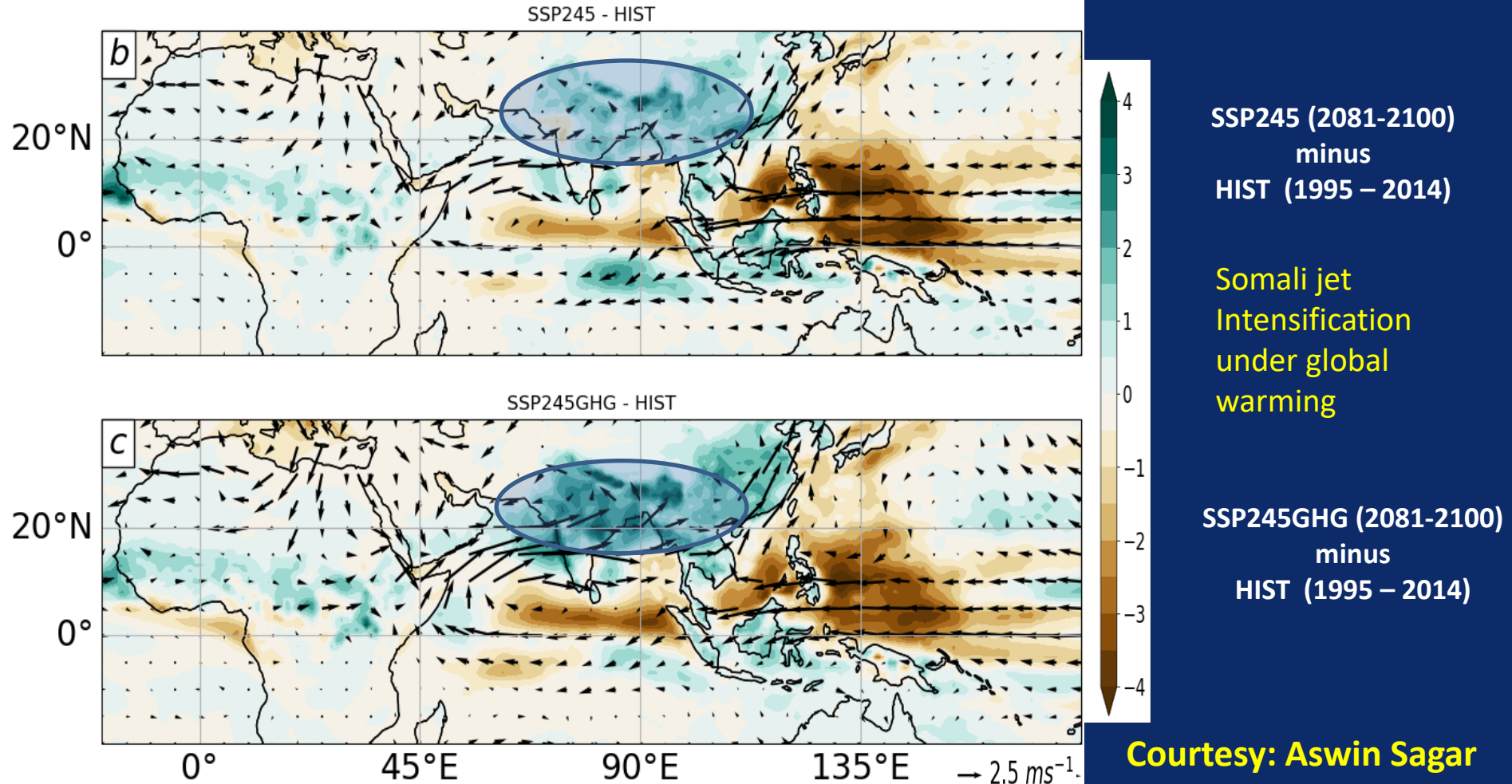
HIST



GPCP & ERA5



Robust strengthening of both monsoon rainfall & cross-equatorial winds under global warming

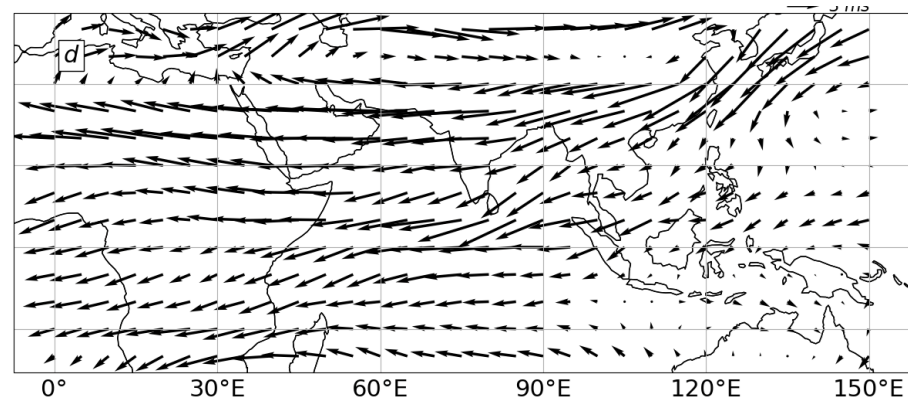
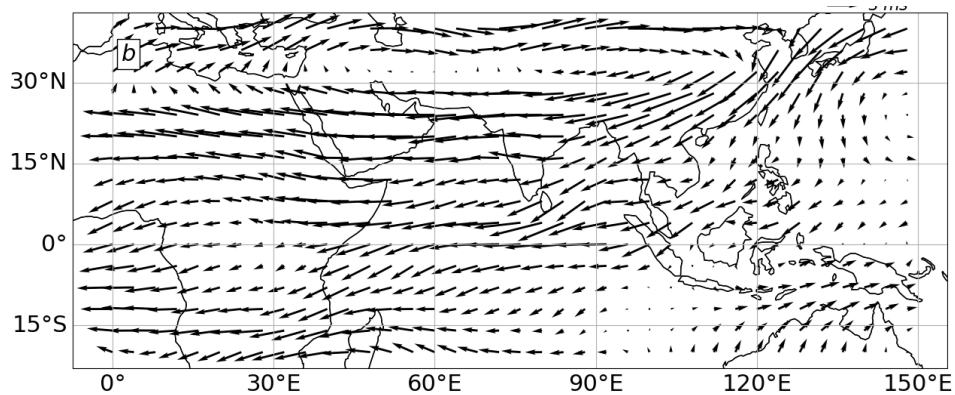


Courtesy: Aswin Sagar

SSP245 - HIST

200 hPa Winds

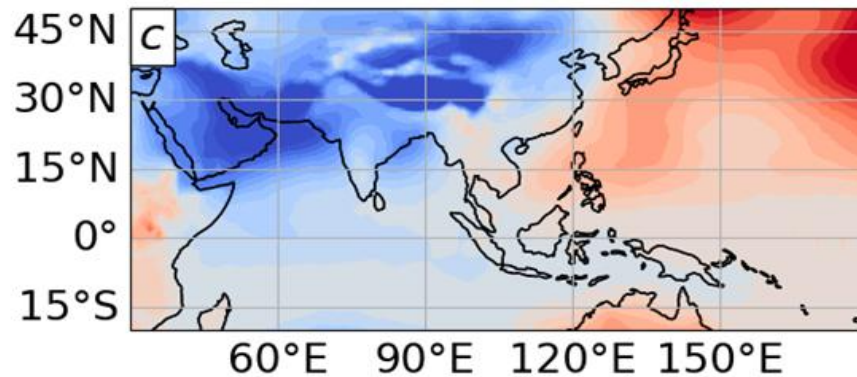
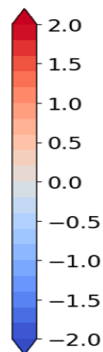
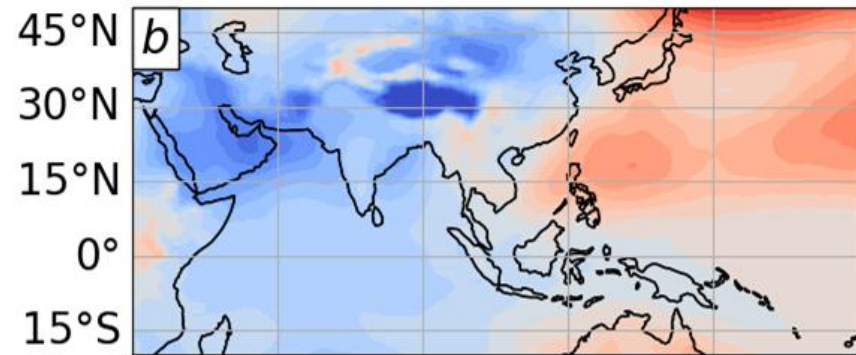
SSP245GHG - HIST



MSLP

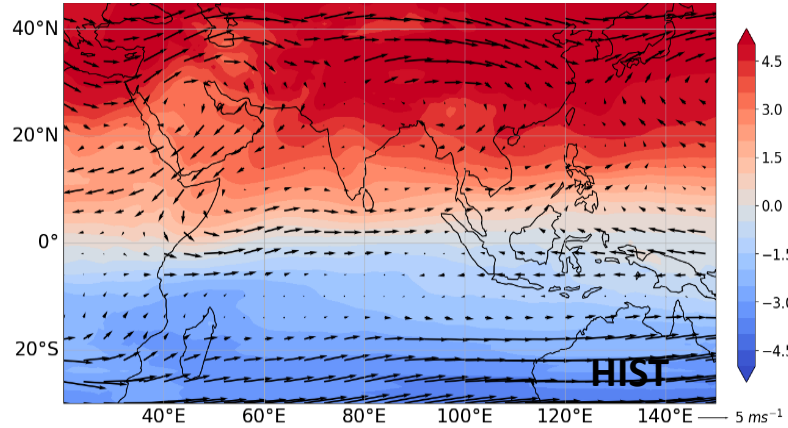
SSP245 - HIST

SSP245GHG - HIST

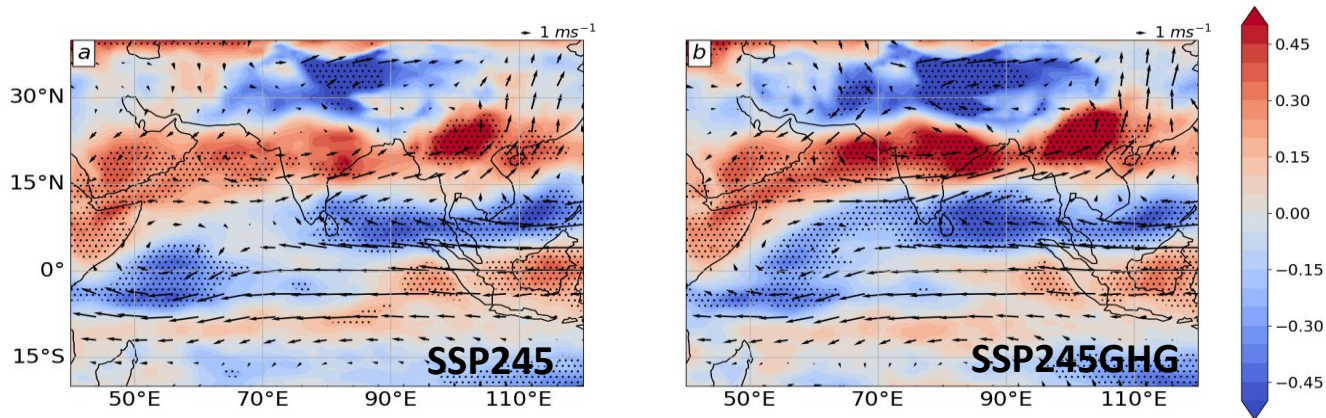


Courtesy: Aswin Sagar

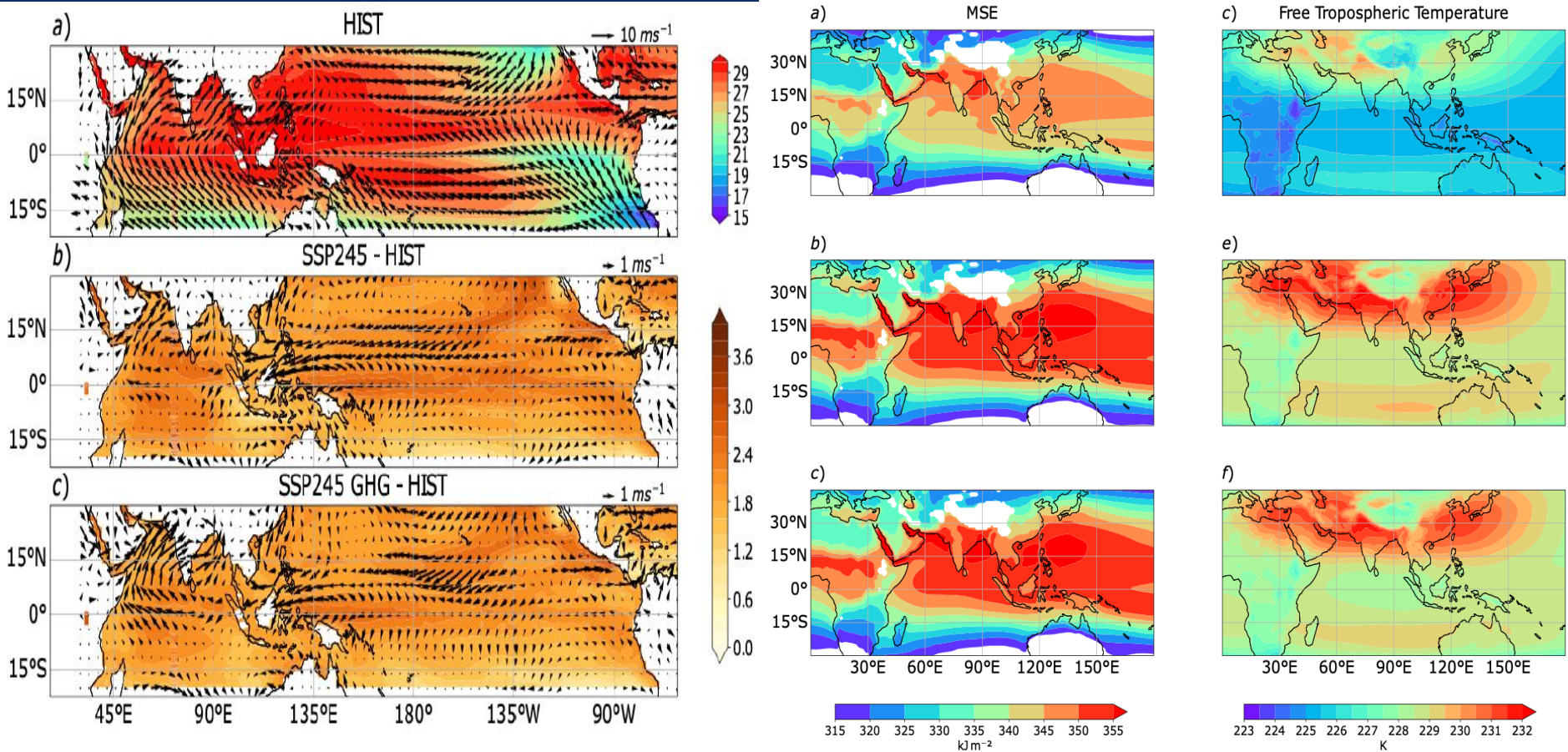
Winds and PV at 500 hPa: HIST (1995-2014)



Change in winds and PV at 500 hPa – (2081-2100) relative to HIST (1995-2014)



Courtesy: Aswin Sagar

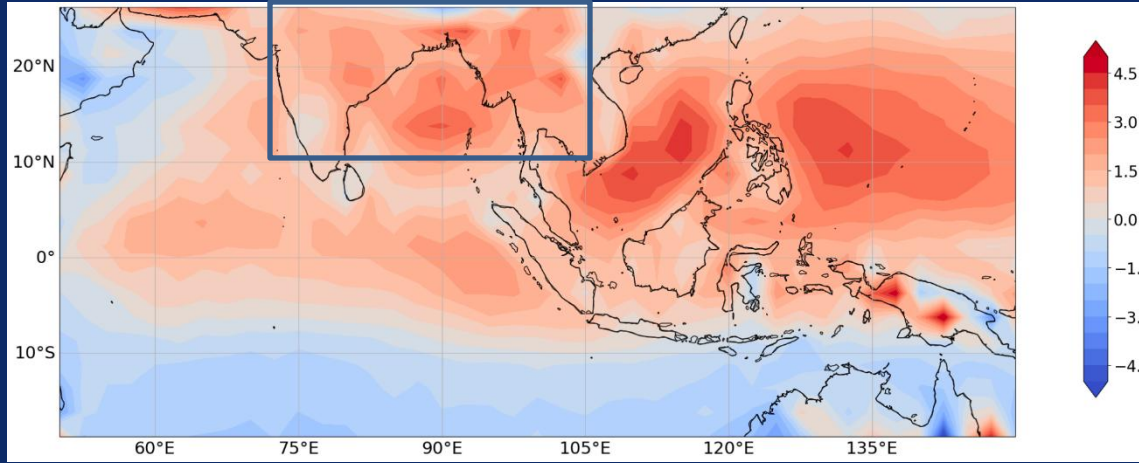


a) Map of JJAS time-mean sea surface temperature (SST, °C) and moisture transport ($\text{kg m}^{-1} \text{s}^{-1}$) from HIST (1995-2014). Difference maps of SST (2081-2100) relative to HIST (1995-2014) b) (SSP245 minus HIST) and c) (SSP245-GHG minus HIST).

Time mean maps of surface moist static energy (MSE) in kJ m^{-2} (left column) and free tropospheric temperature averaged between 450 hPa and 100 hPa in K (right column) for HIST (1995-2014) in (a, d); SSP245 (2081-2100) in (b, e); SSP245-GHG (2081-2100) in (c, f).

Courtesy: Aswin Sagar

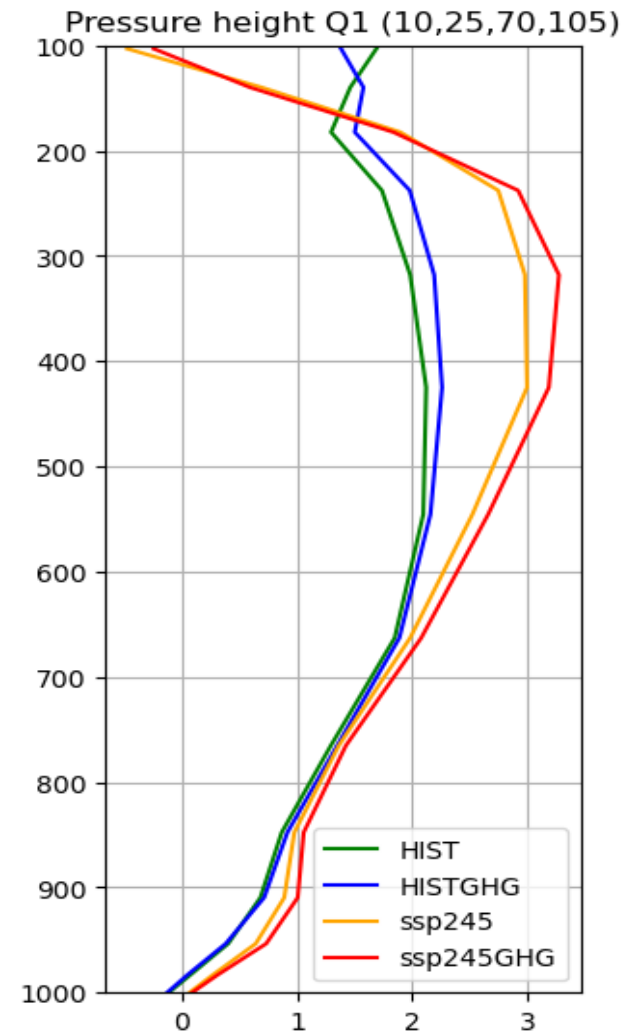
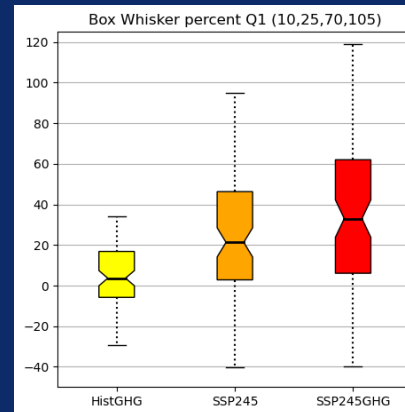
JJAS time-mean (1995-2014) vertically averaged apparent heat source (Q1) from 750 hPa to 200 hPa from HIST



Apparent Heat Source (Q_1) & Apparent Moisture Sink (Q_2) – Yanai et al. 1973, Yanai and Johnson, 1993, Li and Yanai, 1996, Yanai and Tomita, 1998

$$Q_1 = C_p \left(\frac{p}{p_0} \right)^\kappa \left(\frac{\partial \theta}{\partial t} + \mathbf{V} \cdot \nabla \theta + \omega \frac{\partial \theta}{\partial p} \right) \quad \text{and} \quad (1)$$

$$Q_2 = -L \left(\frac{\partial q}{\partial t} + \mathbf{V} \cdot \nabla q + \omega \frac{\partial q}{\partial p} \right). \quad (2)$$

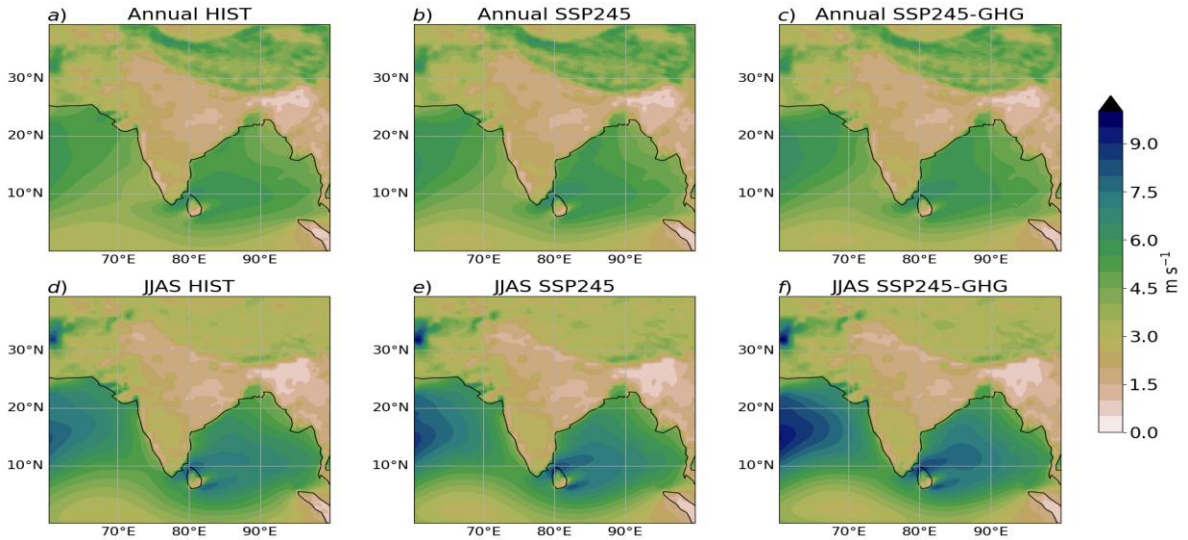


Variables related to the Indian summer monsoon circulation (70E-105E, 10N-30N)

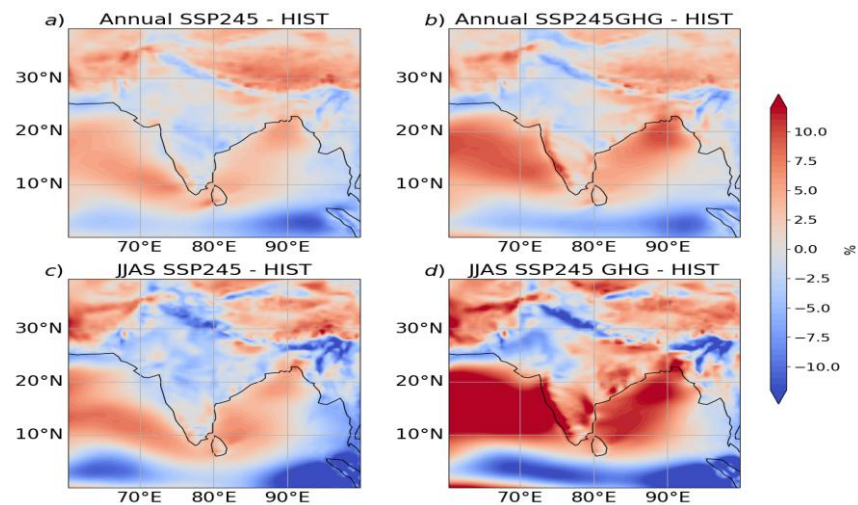
HIST, (SSP245 – HIST), (SSP245GHG – HIST)

Variables	HIST	Δ (SSP245)	Δ (SSP245 GHG)
Precipitation	6.9 mm/day	12.5 %	24.16 %
Omega * (-1)	0.029 Pa/S	22.3 %	36.02 %
Precipitable water	46.78 kg/m ²	1.94 %	4.38 %

Courtesy: Aswin Sagar

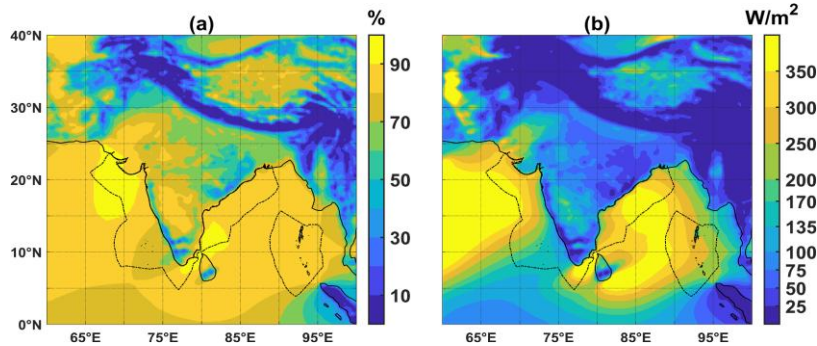


Wind speed at 10 m



**Projected changes (%) in wind speed
relative to HIST**

Wind Power Potential over India using the ERA5 reanalysis – Sai Krishna Sakuru & M.V. Ramana (2023)



Wind energy potential is higher in the off-shore EEZ region (annual mean of $254 W/m^2$; $\sim 2.2 \times 10^{-3}$ GWh/ m^2 per annum) than in the mainland (annual mean of $74 W/m^2$; $\sim 0.65 \times 10^{-3}$ GWh/ m^2). Gujarat state is rich in wind resources (annual mean of $150 W/m^2$), followed by Puducherry, Rajasthan, Karnataka, Andhra Pradesh & Telangana.

It is estimated that 7,204 GW (18,389 GW) of power can be harnessed solely from wind over India's mainland (EEZ) regions, assuming 3% of the area is utilized for this purpose. These numbers comfortably exceed the projected annual gross electricity production of 2.4×10^6 GWh to 2.7×10^6 GWh by 2030. Our projections based on data available till 2020 indicate that electricity generation from renewables (wind) may account for about 22 % (5 to 6.7 %) of India's total electricity generation in 2030.

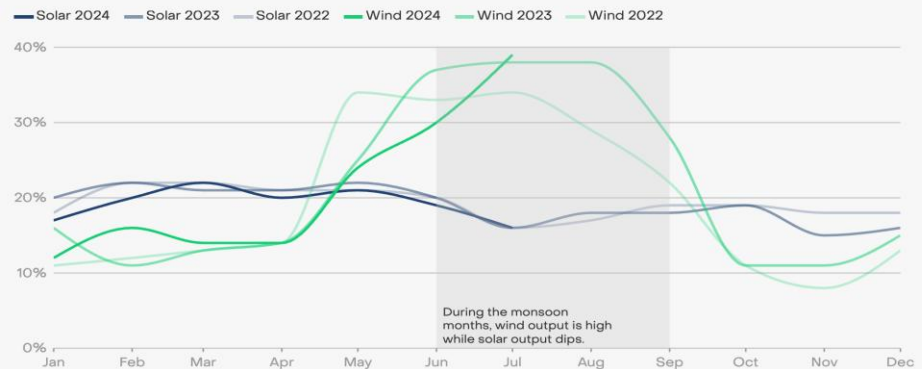
The authors estimated the wind energy potential at 100 m above the surface using nearly four decades of historical wind speed data (1979 - 2018) from the recently available ERA5 reanalysis. The wind speed frequency distribution, which is relevant for choosing the optimal turbine model from a techno-economic aspect, was modelled using a Weibull mixture distribution.

Significant variability in wind speeds over the annual cycle, up to 50 % of the annual mean, is often observed, which can significantly affect the harvestable wind power. Further, winds within the operational range for wind turbines (3 to 25 m/s) occur over inland areas for more than 60 % of the year only over the windiest regions, in contrast to the off-shore areas (more than 70 % of the year).

The generated wind power density maps indicate comparatively higher values during the monsoon season, both over mainland & off-shore regions.

India's wind power output is high during low solar monsoon months

Average capacity factors of solar and wind power since 2022



Source: Ember's analysis based on the Central Electricity Authority installed capacity and generation data

Summary

- Human-induced climate change is already affecting weather & climate patterns in every region of the globe.
- **Indian Summer Monsoon (ISM):** Complex dynamical system involving mutual / coupled interactions of the Land-Ocean-Atmosphere components on different space and time-scales. Robust interactions among Indian monsoon circulation (winds), precipitation, ocean circulation & biogeochemical processes.
- **ISM** changes over the 20th century influenced by anthropogenic emissions of greenhouse gases (GHG) and aerosols. Increases in the monsoon precipitation due to warming from GHG emissions were counteracted by decreases in monsoon precipitation due to cooling from human-caused aerosol emissions. As the climate continues to warm, the ISM precipitation is projected to increase during the 21st century (IPCC AR6)
- **Monsoon wind response to global warming in the LMDz4 (zooming over South Asia) atmospheric GCM**
 - Substantial increase of monsoon precipitation over the subcontinent
 - Robust strengthening monsoon cross-equatorial flow and low-level Somali Jet (CQE framework)
 - Intensification of the vertical gradient of apparent heat source (Q1)
 - Enhanced mid-tropospheric cyclonic PV and vertical velocity
 - Strengthening of monsoon wind speed has **implications for wind energy generation**
- **Future plan:** Coupling of LMDz (zoomed setup) global atmospheric model and ocean model. Very important tool to investigate Monsoon dynamics, Indian Ocean Circulation and Marine Biogeochemical interactions in a changing climate

*Thank you for your
kind attention !*